Study of hybrid photovoltaic module characteristics under local nonuniformity of irradiation and partial shading

© V.M. Emelyanov, S.A. Levina, M.V. Nakhimovich, M.Z. Shvarts

Ioffe Institute, St. Petersburg, Russia
E-mail: vm.emelyanov@mail.ioffe.ru

Received May 12, 2023
Revised July 26, 2023
Accepted October, 30, 2023

The effect of shading and locally increased irradiance of a planar circuit based on *c*-Si solar cells (SCs) as part of a hybrid photovoltaic module was investigated. It was found out that the magnitude and orientation of the shadow on the surface of *c*-Si SCs lead to a change in its efficiency within 1 abs.%, which may be explained by a change in the balance of resistive losses. The presence of high-irradiance areas on the surface of *c*-Si SCs up to 5 mm in diameter (which matches the size of the concentrator A^3B^5 SC) does not have a noticeable effect on the planar circuit yield which remains close to the values characteristic of the conversion of diffuse radiation only.

Keywords: hybrid concentrator-planar photovoltaic module, multijunction solar cell, planar photoconverter, diffusely scattered radiation, shading.

DOI: 10.61011/TPL.2023.12.57580.108A

Hybrid photovoltaic modules (HPVMs) based on multijunction A^3B^5 heterostructure solar cells (SCs), optical concentrators, and also on silicon photoconverters, remain efficient sources of energy under both the clear and cloudy weather conditions. Such modules provide conversion of direct solar radiation by concentrator photovoltaic cells and that of diffuse (scattered) radiation by planar SCs[1–3].

A topical task arising in creating photovoltaic installations with HPVMs is to ensure the planar *c*-Si SCs stability under the condition of a local unevenness of irradiance (energy illumination), for instance, in the case of shading their surfaces [4–6]. Thereat, the effects associated with the emergence of ultra-high irradiance spots (light flares) on the surface of a planar SC in HPVM also turn out to be significant.

The emergence of an ultra-high irradiance spot on the surface of a planar circuit SC may be initiated by a damage of the optical concentrator, reflection of solar radiation from foreign objects with mirror-like surfaces, or slow response or failure of the tracking system, which leads to the focal point shift to the planar SC surface.

The goal of this work was studying the influence of these effects on the HPVM electrical power.

The design of the studied hybrid module (Fig. 1, *a*) was, in general, similar to that presented in [3]. It included four optical concentrators of the „Fresnel lens“ type each 40×40 mm in size, which focused radiation on four small-size GaInP/Ga(In)As/Ge SCs, and also a *c*-Si SC with a passivated emitter and rear contact (PERC). The investigated planar SC was 80×79 mm in size (Fig. 1, *b*) and was one fourth of the TSSB9 module [7]. Optical concentrators jointly with the GaInP/Ga(In)As/Ge SCs formed the concentrator circuit of the module, while those with the *c*-Si SC formed the planar circuit. Average transmittance of the Fresnel lenses was 90% in the SC operating range, the total shading of the *c*-Si SC surface by the concentrator circuit components (SC, current-collecting busbars and radiators) was 12%.

Spectral and current-voltage (JV) characteristics were measured for the *c*-Si SC under study in the concentration factor range of (0.1−1.4)X. At the concentration factors of up to 0.5X, the experimental JV characteristics were well describable by the lumped-parameter model. In the concentration factor range of (1.0−1.4)X, nonlinear losses in the series resistance became significant, correct accounting for which required the use of a distributed equivalent circuit [8,9].

Based on the experimentally measured load JV characteristics, parameters of the $p-n$- junction and series resistance of the *c*-Si SC were determined; they are listed in the table.

The effect of partial shading of *c*-Si SC on its efficiency was studied experimentally using continuous-combustion simulator SS80AA Yamashita Denso (AM1.5G). SC was irradiated from the front side with the flow of 100 W/m^2 (0.1X) to 1400 W/m^2 (1.4X). Shading of the *c*-Si SC working surface was simulated by applying opaque rectangular screens directly to the SC surface in two orientations, namely, parallel or perpendicular to the contact grid busbars, with gradually increasing the shaded part of the surface (Fig. 2, *a*). It has been established that, when the irradiance is 100 W/m^2 (simulation of the mode of the diffuse radiation arrival), shading leads to an efficiency decrease within one absolute percent due to a decrease in the total light power on SC, deterioration in the thermodynamic conversion mode, and decrease in the operating voltage. At the same time, the efficiency behavior at 1000 W/m^2 (total flow of the terrestrial solar radiation) appears to be different and dependent on the shade orientation.

When SC is shaded parallel to the busbars, a slight increase in efficiency is observed due to the contact grid

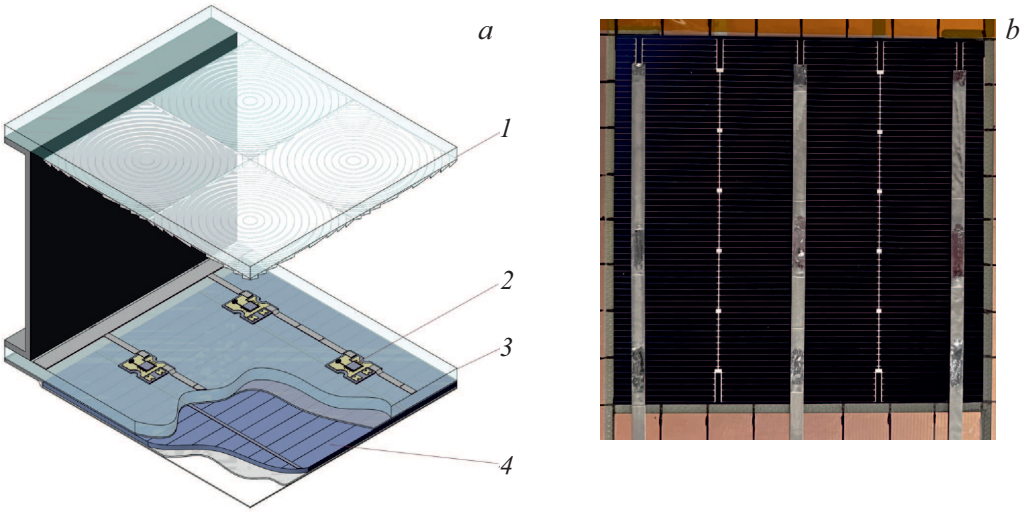

Figure 1. Schematic illustration of the HPVM under study (*a*) and image of the *c*-Si SC included in it (*b*). *1* — Fresnel lenses (silicone) on a glass base, *2* — concentrator *c*-Si SC, *3* — glass base, *4* — *c*-Si SC.

Parameters of the studied *c*-Si SC

Parameter	Value
Density of the front-side irradiation photocurrent (AM1.5G, 1000 W/m^2), mA/cm^2	40.83
Density of the rear-side irradiation photocurrent (AM1.5G, 1000 W/m^2), mA/cm^2	30.77
Injection current density, A/cm^2,	$1.5 \cdot 10^{-13}$
Recombination current density, A/cm^2	$6.5 \cdot 10^{-9}$
Specific series resistance, $\Omega \cdot$ cm^2	2.05
Front-side irradiation efficiency (AM1.5G, 1000 W/m^2), %	20.64
Front-side irradiation efficiency (AM1.5G, 100 W/m^2), %	19.59

„unloading“ and reduction in the forward bias current (injection and recombination) through the $p-n$-junction at the same voltage: when the current flows in the shadowed region, the voltage at the $p-n$-junction appears to be lower (compared to the irradiated region) by twice the value of its drop in the contact grid. In turn, when the shadow is applied perpendicular to the busbars, the mode of forward-bias current flowing is identical to that in a fully irradiated SC, and voltage at the $p-n$-junction in the SC shaded region differs only slightly from that in the irradiated part. If the shadow is applied from the edge (the SC shading factor being $\sim 12-25\%$), then a slight decrease in efficiency is observed. In this mode, no noticeable unloading of the busbars occurs, and a significant photocurrent flows through the shaded area, a part of which is drawn away by forward-bias current through the $p-n$-junction.

The HPVM specific output power was calculated for the circuits based on a planar *c*-Si SC (see the Table) and concentrator GaInP/Ga(In)As/Ge SCs. The concentrator circuit efficiency was 29% at 900 W/m^2.

The simulation results are presented in Fig. 2, *b*. In calculations, the integral power of diffuse radiation was assumed to be 100 W/m^2, photocurrent of the *c*-Si SC was calculated as

$$J_{ph} = \frac{e(1-\xi)}{hc} \int_{\lambda_{\min}}^{\lambda_{\max}} \lambda Q_e^f(\lambda)\Gamma(\lambda)d\lambda + \frac{e(1-\eta)}{hc} \int_{\lambda_{\min}}^{\lambda_{\max}} \lambda Q_e^b(\lambda)\Gamma(\lambda)d\lambda, \quad (1)$$

where $Q_e^f(\lambda)$, $Q_e^b(\lambda)$ are the external quantum yields of photoconductive response in the cases of light irradiation from the front and rear surfaces, $\Gamma(\lambda)$ is the irradiance spectral density in case of diffuse radiation, $\lambda_{\min}-\lambda_{\max}$ is the *c*-Si SC sensitivity range, ξ is the front-surface shading factor, $\eta = 1-(1-\gamma)A$ is the rear-surface effective shading factor, γ is the geometric shading factor, A is the underlying

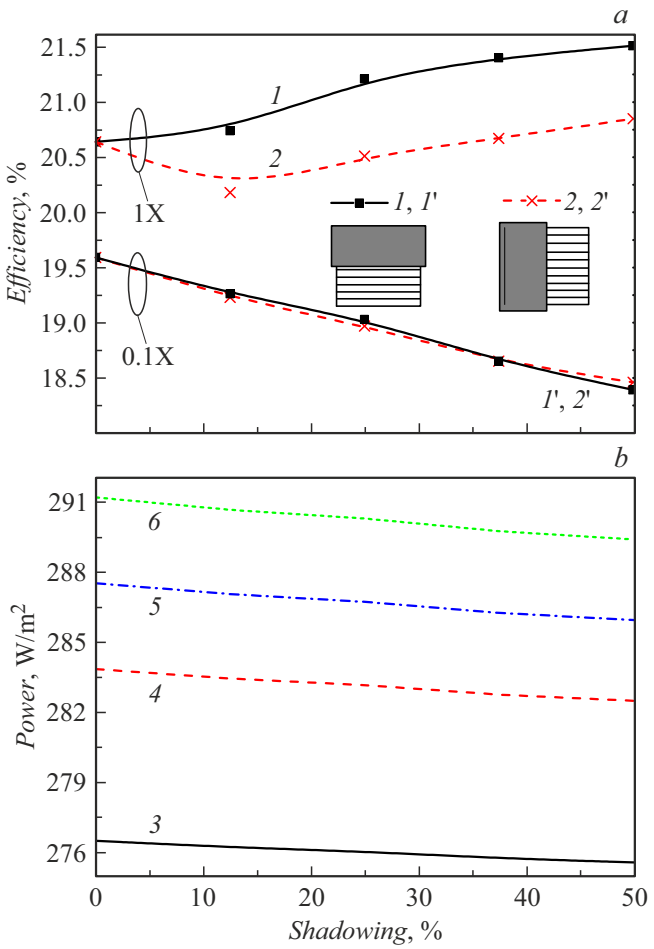

Figure 2. The *c*-Si SC efficiency (*a*) and HPVM specific power (*b*) versus the shading factor. *1*, *1'* — shading parallel to the *c*-Si SC busbars, *2*, *2'* — shading perpendicular to the busbars, *3* — single-facial *c*-Si SC, *4*–*6* — bifacial *c*-Si SC at effective rear-surface shading factors $\eta = 0.5$ (*4*), 0.25 (*5*) and 0 (*6*).

surface albedo, e is the electron charge, h is the Planckś constant, c is the light velocity.

To clarify the effect of flares on the efficiency of solar radiation conversion with a HPVM planar circuit, there was simulated the dependence of specific power of the front-contact and rear-contact planar circuits on the high-irradiance spot diameter (Fig. 3).

Radiation that has passed through the 2×2 module of lens concentrators gave rise to four spots on the surface of studied *c*-Si SCs; total integral power of those spots was 5.2 W at the 900 W/m^2 power density of direct radiation falling on HPVM (Fig. 3). When the spots are small, the planar circuit output power differs only slightly from the same characteristic in the case of converting only diffuse radiation. With increasing spot size, the output power approaches value 1000 W/m^2 (AM1.5G) corresponding to the case of converting the total radiation flux. Since the pattern of the *c*-Si SC contact grid is not optimized for converting the concentrated solar radiation, a significant decrease in the planar circuit efficiency is observed in the case of a small flare area because of an increase in ohmic losses within the high-irradiance spot.

A more source of the efficiency reduction in the event of the light spot emergence on the SC surface may be an increase in the SC temperature in the high-irradiance region. However, no significant temperature gradient and, hence, no its effect on the efficiency was observed for the studied *c*-Si SCs at all the considered spot parameters. In the case of ambient temperature of 25°C and natural convective cooling of HPVM, the temperature at each point of the *c*-Si SC surface remained within the 60–70°C range in all the modes. Displacement of the high-irradiance spot over the *c*-Si SC surface also did not affect the electric power. This

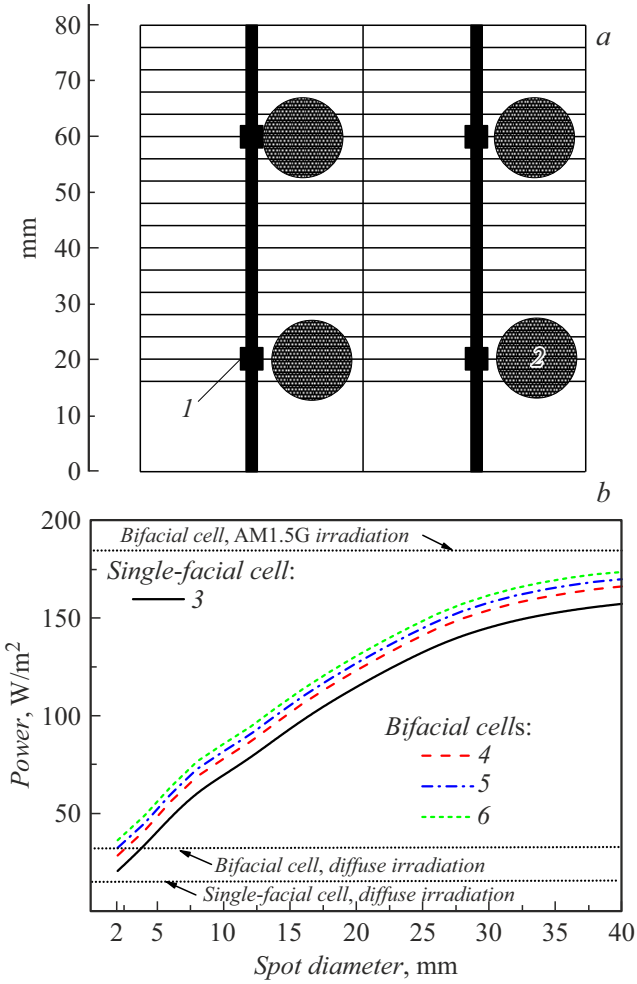

Figure 3. *a* — schematic illustration of emergence of high-irradiance spots on the *c*-Si surface. *1* — the GaInP/Ga(In)As/Ge SC position, *2* — high-irradiance spot. *b* — output power of the HPVM planar circuit versus the flare spot size. *3* — power of the single-facial *c*-Si SC; *4*–*6* — power of the bifacial *c*-Si SC at effective rear-surface shading factors $\eta = 0.5$ (*4*), 0.25 (*5*) and 0 (*6*). The dashed lines represent the planar circuit output power during converting flows of the total radiation (1000 W/m^2) and diffuse radiation (100 W/m^2) (two lower lines, ~ 30 and ~ 15 W/m^2) with accounting for the optical concentrator losses and losses for HPVM shading.

is due to that the ohmic loss increase with increasing local light load proceeds faster in the semiconductor SC layers than in the busbars.

Thus, in the case of the diffuse radiation conversion, shading of the planar circuit results in the yield reduction according to a law somewhat stronger than linear because of both the decrease in the converted light flux and slight decrease in the *c*-Si SC efficiency. Emergence of high-irradiance regions on the *c*-Si SC surface does not deteriorate the HPVM planar circuit characteristics, but yet does not make a significant positive contribution to its power yield. The increase in the high-irradiance spot size to 30 mm makes the HPVM planar circuit yield closer to the yield of an isolated *c*-Si SC under the same conditions.

Funding

The study was supported by the Russian Science Foundation, project № 22-19-00158 (https://rscf.ru/project/22-19-00158/).

Conflict of interests

The authors declare that they have no conflict of interests.

References

[1] *High-efficient low-cost photovoltaics*, ed. by V. Petrova-Koch, R. Hezel, A. Goetzberger. Springer Ser. in Optical Sciences (Springer, Cham, 2020), vol. 140. DOI: 10.1007/978-3-030-22864-4
[2] J.F. Martínez, M. Steiner, M. Wiesenfarth, T. Fellmeth, T. Dörsam, M. Wiese, S.W. Glunz, F. Dimroth, Prog. Photovolt.: Res. Appl., **28** (5), 349 (2020). DOI: 10.1002/pip.3239
[3] M.Z. Shvarts, A.V. Andreeva, D.A. Andronikov, K.V. Emtsev, V.R. Larionov, M.V. Nakhimovich, P.V. Pokrovskiy, N.A. Sadchikov, S.A. Yakovlev, D.A. Malevskiy, Tech. Phys. Lett., **49** (2), 50 (2023). DOI: 10.21883/TPL.2023.02.55371.19438.
[4] J.P.N. Torres, S.K. Nashih, C.A.F. Fernandes, J.C. Leite, Energy Syst., **9** (1), 195 (2018). DOI: 10.1007/s12667-016-0225-5
[5] S. Wendlandt, A. Drobisch, D. Tornow, M. Friedrichs, S. Krauter, P. Grunow, in *Proc. ISES Solar World Congress 2011* (Kassel, Germany, 2011), p. 120. DOI: 10.18086/swc.2011.14.18
[6] A. Atia, F. Anayi, M. Gao, Energies, **15** (23), 9067 (2022). DOI: 10.3390/en15239067
[7] *TSEC TSSB9 c-Si solar cell datasheet.* https://www.tsecpv.com/upload/website/battery/download/M69BB_B9.pdf
[8] V.M. Emelyanov, S.A. Mintairov, S.V. Sorokina, V.P. Khvostikov, M.Z. Shvarts, Semiconductors, **50** (1), 125 (2016). DOI: 10.1134/S1063782616010085.
[9] V.M. Emelyanov, N.A. Kalyuzhnyy, M.A. Mintairov, S.A. Mintairov, M.A. Shvarts, V.M. Lantratov, in *Proc. of the 25th European Photovoltaic Solar Energy Conf. and Exhibition (EPSEC)* (Valencia, Spain, 2010), p. 1DV.2.33. DOI: 10.4229/25THEUPVSEC2010-1DV.2.33

Translated by Ego Translating